Korean J. Chem. Eng., 40(7), 1715-1724 (2023)
DOI: 10.1007/s11814-023-1399-x

pISSN: 0256-1115
eISSN: 1975-7220

Molecular encapsulation of nortriptyline in the β-cyclodextrin cavity: *In-vitro* cytotoxic potential against MCF-7 cell line

Rajaram Rajamohan[*,‡,†], Muthusamy Viswalingam[,‡], Yong Rok Lee[*,†], Samikannu Prabu[***], and Krishnamoorthy Sivakumar[****]**

*School of Chemical Engineering, Yeungnam University, Gyeongsan 38541, Korea
**Department of Chemistry, Periyar Maniammai Institute of Science and Technology, Thanjavur - 613 403, India
***Department of Chemistry, P.S.V College of Engineering and Technology, Krishnagiri - 635 108, India
****Department of Chemistry, Sri Chandrasekharendra Saraswathi Viswa Mahavidyalaya (Deemed University), Kanchipuram - 631 561, India

(*Received 15 November 2022 • Revised 18 January 2023 • Accepted 31 January 2023*)

Abstract−In the liquid state, UV-visible and fluorescence spectroscopy was used to examine the inclusion complexes of nortriptyline (NP) and β-cyclodextrin (β-CD). The degree of inclusion complexation causes NP's absorbance and fluorescence intensity to be significantly increased during interaction with β-CD. The binding constant was determined by UV-VIS and fluorescence spectroscopy, and the results indicated a 1 : 1 stoichiometry for the inclusion complex at 303 K. Complexation is a spontaneous and exothermic process, as determined by Gibbs's free energy change. To produce solid inclusion complexes (ICs), mixing and co-precipitation were used, which were then characterized using Fourier-transform infrared spectroscopy (FT-IR), scanning electron microscope (SEM), X-ray powder diffraction (XRD), and thermogravimetric analysis/differential scanning calorimetry (TGA/DSC). According to molecular docking studies, the aromatic ring of the NP does not penetrate the secondary hydroxyl rim of the β-CD cavity, but the aliphatic part of the NP trapped in the cavity is more thermodynamically advantageous. NP and NP : β-CD-ICs were screened for *in vitro* cytotoxicity on Michigan Cancer Foundation-7 (MCF-7) cell line using the 3-(4,5-dimethylthiazol-2-yl)-2,5-diphenyl-2H-tetrazolium bromide (MTT) assay, and the results showed that the cytotoxicity was not affected by creating an ICs.

Keywords: Nortriptyline, β-Cyclodextrin, Inclusion Complex, Docking Study, *In-vitro* Cytotoxic Assay

INTRODUCTION

Among the most popular medications for smoking cessation, nortriptyline hydrochloride is a second-generation tricyclic antidepressant that is effective for treating endogenous depression, as well as some cases of reactive depression [1]. In particular, tricyclic antidepressants (TCAs), such as amitriptyline and desipramine, which are commonly used to treat depression and chronic pain [2,3], also have antineoplastic activity in a wide variety of cancer cells [4-8]. Similarly, nortriptyline also exhibits anticancer activity in several different types of cells [9,10]. By creating inclusion complexes with the host-guest system, a broad concept of intermolecular interactions can be understood [11,12]. Generally, cyclodextrin has high confidence that inclusion complexes can develop, particularly with molecules whose structures are acceptable [13]. Sugar molecules that are linked together in a ring are called cyclodextrins. For instance, there is a glucopyranoside unit found in β-CD. It is well known that β-CD can form inclusion complexes with a variety of compounds. There are several hydroxyl groups on the surface of the β-CD, so it is very hydrophilic.

Consequently, β-CD forms inclusion complexes with a wide selection of hydrophobic molecules and molecules of appropriate polarity and size [14]. A primary focus of their pharmaceutical applications is the ability to increase the solubility, stability, and bioavailability of drugs [15], as well as the ability to regulate drug release [16], both of which can have much potential, and uses in drug formulations. Taking up a molecule in its entirety or in part, the β-CD can create inclusion complexes with a variety of guest molecules [17,18]. Solid or liquid encapsulation of molecules is possible. Researchers are developing liquid inclusion complexes in order to increase fluorescence intensity in biological specimens [19-23]. Included complexes are formed due to electrostatic interactions, hydrogen bonds, conformational strain release, and charge-transfer interactions [24].

It is expected that the inclusion complexation of NP with β-CD in an aqueous solution will have a significant impact in this study, where the stoichiometry of β-CD and NP was determined through UV and fluorescence spectral methods. The incorporation of CDs in complexes with pharmaceuticals or pesticide molecules, which may be of use in the insecticide, food, and pharmaceutical industries, was recently discovered [25]. A cell line of human breast cancer, MCF-7, was used to test the cytotoxicity of pure and solid complexes of their compounds.

†To whom correspondence should be addressed.
E-mail: rajmohanau@yu.ac.kr, yrlee@yu.ac.kr
‡Equally Contributed.

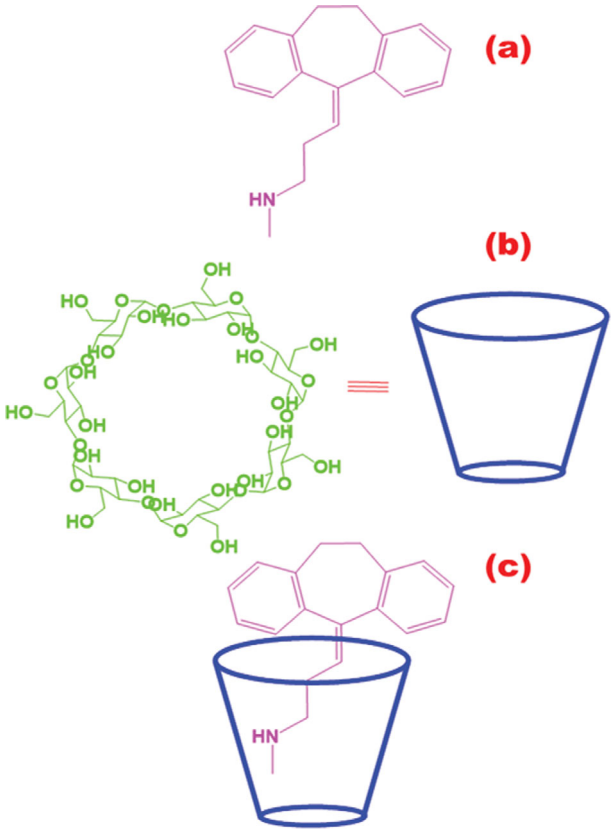

Scheme 1. Structures of (a) NP (b) β-CD and (c) NP : β-CD-ICs.

MATERIALS AND METHODS

1. Materials

Sigma-Aldrich provided NP and β-CD, which were used as directed. All experimental solutions were made with double distilled water. The rest of the chemicals and solvents were of the highest quality (Spectro grade). Neither β-CD nor NP was further purified before use in the assays. We maintained a pH of 6.5 in the test solution. Concentrations of the stock solution of NP and β-CD were prepared as 3×10^{-4} M and 0-12×10^{-3} M, respectively. Analysis was carried out such as UV-Vis and fluorometric measurements for the solutions, which were prepared just prior to doing the same.

Ethylenediaminetetraacetic acid (EDTA), glucose, and antibiotics were supplied by Hi-Media Laboratories Ltd., Mumbai. Sigma Aldrich Co., St Louis, USA, provided Fetal Bovine Serum (FBS), Phosphate Buffered Saline (PBS), Dulbecco's Modified Eagle's Medium (DMEM), and Trypsin. Hi-Media Laboratories Ltd., Mumbai, provided fetal bovine serum (MTT), fetal bovine serum (F DMSO and propanol provided by E. Merck Ltd., Mumbai, India.

2. Preparation of ICs in Solutions

The samples were prepared with a steady concentration of NP and varying concentrations of β-CD (Scheme 1). The concentration of the NP solution was kept constant at 3×10^{-4} M, while the concentration of the β-CD solutions was changed from 2.0 to 12.0×10^{-3} M. To get the NP : β-CD solutions to equilibrium, they were shaken vigorously for six hours. Studies were conducted mostly at room temperature.

3. Preparations of ICs in Solid-state

Through the co-precipitation of NP and β-CD with a 1 : 1 molar ratio, solid ICs between them were synthesized [26,27]. The weight of NP was changed slightly in the synthetic procedure, as the molecular weight differs to get a 1 : 1 ratio. There is an exact 1 : 1 molar ratio between NP and β-CD. Water is used to prepare a saturated solution of β-CD and NP, which is then slowly mixed together in a conical flask until a suspension is formed. After stirring for 30 minutes at 40 °C, the suspension is kept stirring at room temperature for 24 hours. Using a refrigerator, it has been possible for the precipitation of solid complexes to settle in an undisturbed environment for up to 12 hours. It revealed that no precipitate had settled at the bottom of the conical flask because the ICs were dissolved in the water, and the freeze dryer was subsequently used to obtain the solid product after evaluation of solvents, such as water and white-colored ash like the product had been obtained. Also, physical mixtures (PMs) were obtained to examine the possibility of IC formation through co-precipitation. NP-β-CD-ICs and PM are the final dried precipitates when the physical mixing and co-precipitation process is completed.

4. Molecular Docking Study

In addition to using the Patch-Dock server to determine the most likely structure of the NP : β-CD-ICs [28], we used molecular docking to determine the structure of the NP : β-CD-ICs as well. We obtained 3D structural data for β-CD and NP from crystallographic databases. NP and β-CD molecules were docked using the Patch-Dock server by submitting their 3D coordinates. For docking, complex settings were used. Patch-Dock uses geometry-based molecular docking to find docking changes that are complementary to molecular shape. Connolly dot surface representations of molecules are divided into concave, convex, and flat patches [29]. To create potential transformations, the geometric fit and atomic desolvation energy scores [30] functions were used to evaluate these divided complementary patches. RMSD (root mean square deviation) clustering of docked solutions was used to select non-redundant results and remove redundant docking structures. The NP molecule's ground state was optimized using the AM1 method.

5. Preparation of the Solutions for *In-vitro* Cytotoxic Study

As part of the cytotoxicity tests, each weighed dose of the test medication was dissolved separately in distilled DMSO and the volume was generated by DMEM supplemented with 2% inactivated FBS filtered to 0.1 mg/ml concentration and then sterilized by dialysis. Serial two-fold dilutions of this were used for cytotoxic investigations. Trypsinization and cell counting were performed at 1.0×10^{5} cells/ml using DMEM containing 10% FBS. Each well of the 96-well microtiter plate was filled with 0.1 ml of the diluted cell suspension (about 10,000 cells). The supernatant was flicked off after 24 hours, the monolayer was washed once with media, and 100 µl of each of the test drug doses was applied to the partial monolayer. A microscopic examination was performed every 24 hours and observations were recorded after three days of incubation at 37 °C in 5% CO_2. Each well was added 50 mL of MTT in PBS after the medication solutions in the wells had been removed after 72 hours. Incubation was in a 5% CO_2 environment at 37 °C for 3 hours. The supernatant was removed and 100 milliliters of propanol was added to the plates before gently agitating them to dissolve the formazan

that had formed. The absorbance was measured using a microplate reader with a wavelength of 540 nm. For each cell line, the dose-response curves were used to calculate the concentrations of drugs required to inhibit 50% of growth (CTC_{50}).

$$\%\ \text{Growth Inhibition} = 100 - \frac{\text{Mean OD of individual test group}}{\text{Mean OD of control group}} \times 100 \quad (1)$$

6. Instruments

The UV-Visible and fluorescence spectral measurements were made on a KJENA model SPECORD 200 PLUS double-beam spectrophotometer, and on a Spectrofluorometer from Perkin Elmer, respectively. For all the samples, pH was determined using a pH meter L1–120, and FT-IR spectra were obtained using a Bruker Optics Alpha-T FT-IR spectrometer fitted with OPUS version 6.5 and using the KBr pellet method, covering the spectral range of 400-4,000 cm^{-1}. With an automated Philips Holland-PW 1710 scanner equipped with a Cu radiation filter, powder XRD patterns were acquired over a range of 10 to 50°/2θ. Molecular imaging was performed with a JEOI-JSM 5610LV scanning electron microscope. Perkin Elmer's Q600 SDT and Q2 diamond systems were used to investigate the thermal properties of the samples.

RESULTS AND DISCUSSION

1. Interaction of NP : β-CD-ICs in Solution

NP with β-CD was examined by absorption spectroscopy to investigate the development of ICs. Adding β-CD to NP alters its absorption spectra at pH 6.5. In Fig. 1, NP is shown at a wavelength of 244.0 nm. Increasing the concentration of β-CD leads to a gradual increase in absorbance with a small shift to the blue. These UV spectral alterations indicate NP and β-CD interactions. NP molecules' β-CD cavity surroundings reduce the polarity of their surroundings, causing a blue shift. Based on these results, we conclude that the hydrophobic interaction between the NP and β-CD promotes NP dissolution via the formation of ICs [31]. Based on these findings, it would appear that the NP and β-CD molecules are forming the homologous ICs.

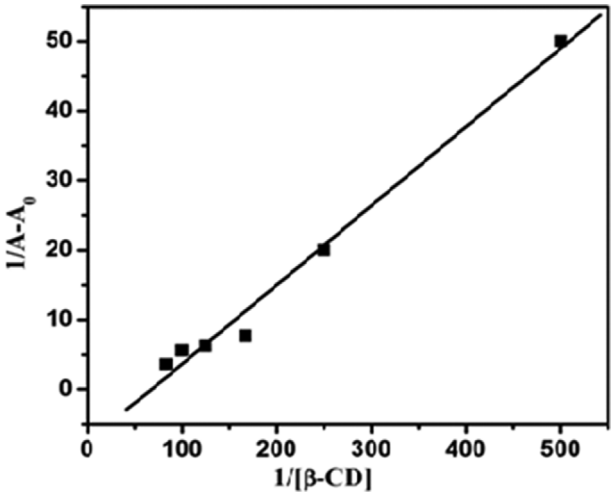

Fig. 2. BH absorption plot of NP with β-CD.

Based on the change in absorbance after adding β-CD to NP, one can use the BH equation to determine the binding constants and stoichiometry of ICs in this system [26,27]. In Fig. 2, $1/(A-A_0)$ is plotted against 1/[β-CD]. There is a strong linear correlation (R^2=0.9935) between NP and β-CD to show 1 : 1 ICs. Eq. (2) can be used to calculate the binding constant (K) for the formation of ICs from the slope of the BH plot. The binding constant at 303 K was estimated to be 32.0 M^{-1} (Table 1).

$$K = \frac{1}{\text{Slope}(A - Ao)} \quad (2)$$

As a function of concentration-dependent β-CD, the fluorescence spectrum of NP is shown in Fig. 3. All experiments used the

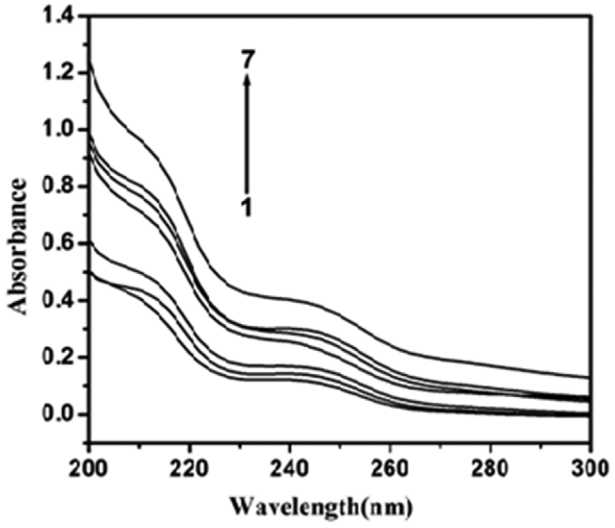

Fig. 1. Absorption spectra of NP (3×10^{-4} M) in β-CD with β-CD (mol·dm^{-3}): 1) Without β-CD, 2) 2×10^{-3}, 3) 4×10^{-3}, 4) 6×10^{-3}, 5) 8×10^{-3}, 6) 10×10^{-3}, 7) 12×10^{-3}.

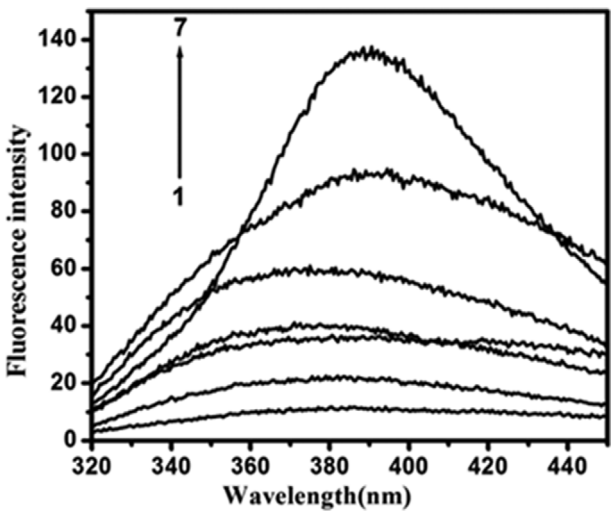

Fig. 3. Fluorescence spectra of NP (3×10^{-4} M) with β-CD [1. Without β-CD, 2. 2×10^{-3}, 3. 4×10^{-3}, 4. 6×10^{-3}, 5. 8×10^{-3}, 6. 10×10^{-3}, 7. 12×10^{-3} M].

Table 1. Thermodynamic parameters

S. No	Parameters	By absorption spectra	By fluorescence spectra
1	Stoichiometry	1 : 1	1 : 1
2	Binding constant (M^{-1})	32	37.12
3	Regression co-efficient (r^2)	0.9935	0.9916
4	Standard deviation	2.28	0.0051
5	ΔG Value ($k{\cdot}J{\cdot}mol^{-1}$)	−8.76	−9.11

same excitation wavelength and different concentrations of β-CD, ranging from 2×10^{-3} to 12×10^{-3} M. To investigate the effect of NP : β-CD-ICs on the fluorescence spectra of NP, it was found that the excitation intensity of NP increases with NP concentration. As a result, NP and β-CD form a stable combination.

Additionally, NP combined with β-CD caused a blue shift in the emission spectrum. When encapsulated with the inner side of the water, the NP guest molecule confronts a much broader range of chemical conditions than the β-CD molecule. As a result, Ramamurthy and Eaton [32] found that the guest molecule's photophysical and photochemical characteristics and properties had been altered. As a result of the blue shift, NP must be exposed to less polar conditions within the hydrophobic cavity of β-CD [33]. In these results, it is clear that the NP is transferred from a more protic environment (cavity of β-CD) to a less protic one.

A prior report [34] confirms that NP : β-CD-ICs form when the concentration of β-CD increases. To examine the NP fluorescence intensity's β-CD dependence, a BH plot can be used [35,36]. $1/(I-I_o)$ is plotted against 1/[β-CD], and good linearity is observed (regression coefficient, R^2=0.9916) (Fig. 4). Based on the plot's linearity, NP : β-CD-ICs have a stoichiometry of 1 : 1. According to the slope of the straight line, K is found to be 37.12 M^{-1} at 303 K.

The binding constant values for the complexes between NP and B-CD in a liquid state with the shifts in absorption and fluorescence spectra were compared and revealed that there are not many differences between them. Comparatively, the binding constant values are low and it is supported by the other complexation with CDs [37]. Already the binding constant value of the acyclovir/H-CD system is found approximately the same as that reported [38]. For acyclovir/H-CD and acyclovir/B-CD, the binding constant values have been reported as 8.0 M^{-1} [39], and 22.0 M^{-1} [40]. The different binding strengths between CD and drug molecules could be caused by the differing substitution degrees (SD) of hydroxypropyl groups in H-CD [41].

From the binding constant value, the Gibbs free energy change (ΔG) may be calculated.

$$\Delta G = -2.303\ RT \log K \quad (3)$$

Under the assumption that the binding constant value K is equal to 32 and 37.12 $kJ{\cdot}mol^{-1}$ in the ground and excited states, the thermodynamic parameter ΔG values are −8.76 and −9.11 $kJ{\cdot}\ mol^{-1}$ in the ground state, respectively (Table 1). NP : β-CD-ICs exist spontaneously at 303 K, as indicated by the negative ΔG values.

2. Interaction of NP : β-CD-ICs in Solid-state

During the interaction of the guest molecule with the host, the molecule is through complexation in the solid state, the absorption bands originating from the included part of the guest molecule are often relocated or may even be altered in terms of peak intensity [42]. FT-IR spectroscopy is used to analyze the ICs obtained by the above-said methods. FT-IR spectra of NP, β-CD, PM, and NP : β-CD-ICs can be seen in Fig. 5. There are several major peaks appearing in the spectral outputs and they are interpreted as

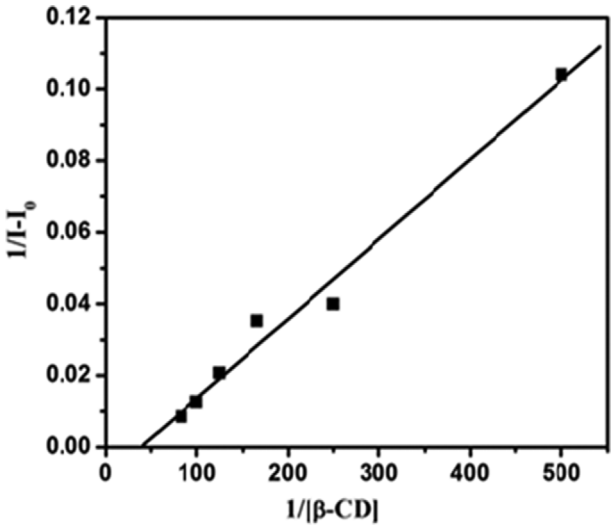

Fig. 4. BH fluorescence plot for 1 : 1 complexation of NP with β-CD.

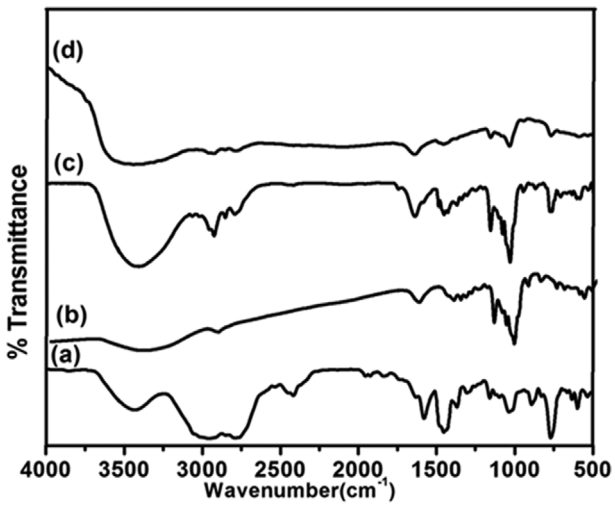

Fig. 5. FT-IR spectra of (a) NP, (b) β-CD, (c) PM, and (d) NP : β-CD-ICs.

secondary amine N-H stretching, aliphatic C-H stretching, aliphatic C-C=C asymmetric stretching, aliphatic C-N stretching, and aromatic C-C=C bending of NP at 3,849.54, 2,956.42, 1,579.15, 1,099.22, 769.98, and 1,452.64 cm^{-1} (Fig. 5(a)), respectively. The -OH group of the β-CD molecule exhibits symmetric and asymmetric stretching vibration due to the numerous intermolecular hydrogen bonds, as denoted by the broad band at 3,380 cm^{-1} (Fig. 5(b)), and another band at 2,920 cm^{-1} corresponds to the C-H stretching vibration. An absorption band at 1,650 cm^{-1} can be attributed to H-O-H bending, whereas absorption peaks at 1,160 and 1,030 cm^{-1} can be attributed to asymmetric and symmetric C-O-C stretching vibrations, respectively.

Figs. 5(c) and 5(d) show the FT-IR spectra of the physical combination and the ICs. The PM's and NP : β-CD-IC's secondary amine N-H stretching frequencies were 3,407.71 and 3,440.29 cm^{-1}, respectively. In NP, the aliphatic C-H stretching frequency is 2,956.42 cm^{-1}, while the values for the PM and solid inclusion complex are 2,924.06 and 2,925.52 cm^{-1}, respectively. Similarly, for PM and NP : β-CD-ICs, the stretching frequencies of other key groups are compared and altered.

Aromatic C-H bending and aromatic C-C=C asymmetric stretching frequencies of the PM and NP : β-CD-ICs show only small shifts (or no significant change). The PM and NP : β-CD-ICs show large alterations in secondary amine N-H stretching, aliphatic C-H stretching, aliphatic C-N stretching, and aliphatic C-C=C symmetric stretching frequencies. For PM and NP : β-CD-ICs, the aromatic C-H bending and aromatic C-C=C asymmetric stretching frequencies are modest shifts, showing that the benzene ring of NP is not entrapped in the hydrophobic cavity of β-CD. Secondary amine N-H stretching, aliphatic C-H stretching, aliphatic C-N stretching, and aliphatic C-C=C stretching are all indicated by substantial variations in frequency. Symmetric for PM and NP : β-CD-ICs, stretching is entrapped in the hydrophobic cavity of β-CD. As a result, for PM and NP : β-CD-ICs, the aliphatic group is exclusively entrapped in the hydrophobic cavity of β-CD.

The FT-IR spectra of the PM and the NP : β-CD-ICs are shown in Figs. 5(c) and 5(d). Secondary amine N-H stretching frequencies for PM and NP : β-CD-ICs were 3,407.71 and 3,440.29 cm^{-1}, respectively. According to NP, the stretching frequency of aliphatic C-H is 2,956.42 cm^{-1}, while the values for the PM and NP : β-CD-ICs are 2,924.06 and 2,925.52 cm^{-1}, respectively. In the same way, the stretching frequencies of other key groups were compared and altered for the PM and NP : β-CD-ICs.

Only small shifts (in other words, no significant change) are observed in aromatic C-H bending and aromatic C-C=C asymmetric stretching frequencies of NP : β-CD-ICs. The frequency of secondary amine N-H stretching, aliphatic C-H stretching, aliphatic C-N stretching, and aliphatic C-C=C symmetric stretching is greatly altered in the PM and NP : β-CD-ICs. A modest shift in the aromatic C-H bending and aromatic C-C=C asymmetric stretching frequencies for NP and ICs indicates that the benzene ring of NP is not trapped in the hydrophobic cavity of β-CD. There are significant variations in frequency associated with secondary amine N-H stretching, aliphatic C-H stretching, aliphatic C-N stretching, and aliphatic C-C=C stretching. In the case of PM and NP : β-CD-ICs, the hydrophobic cavity of β-CDs encloses the aliphatic group exclusively.

SEM is one of the secondary results of the investigation of the surface roughness and surface texture of the substances with NP using β-CD [43,44]. Fig. 6 shows the microscopic characteristics

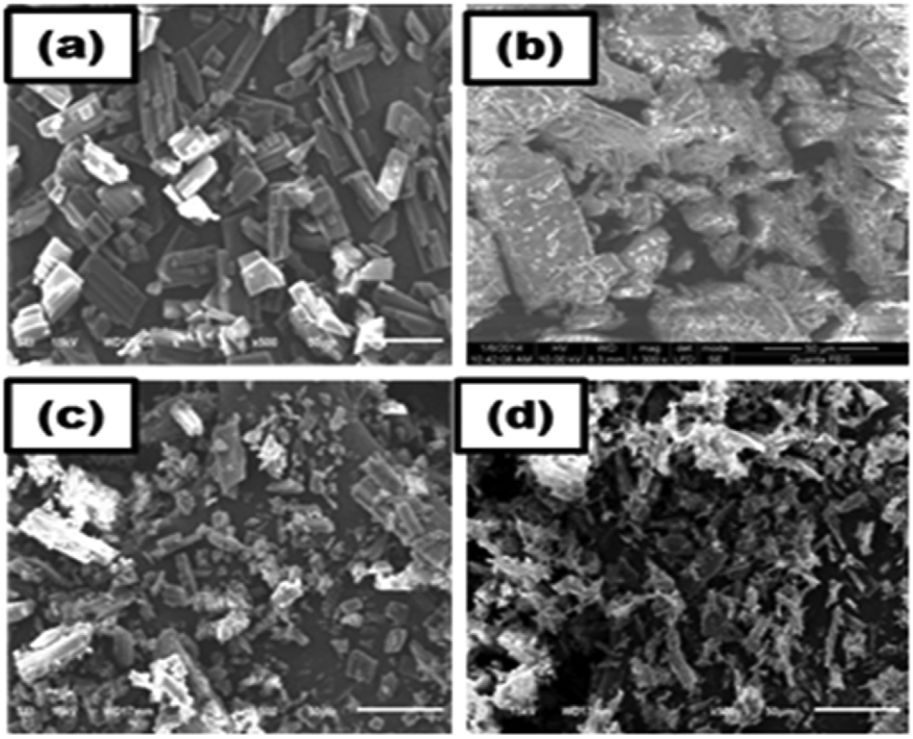

Fig. 6. SEM images of (a) NP, (b) β-CD, (c) PM, and (d) NP : β-CD-ICs with ×10,000 magnifications.

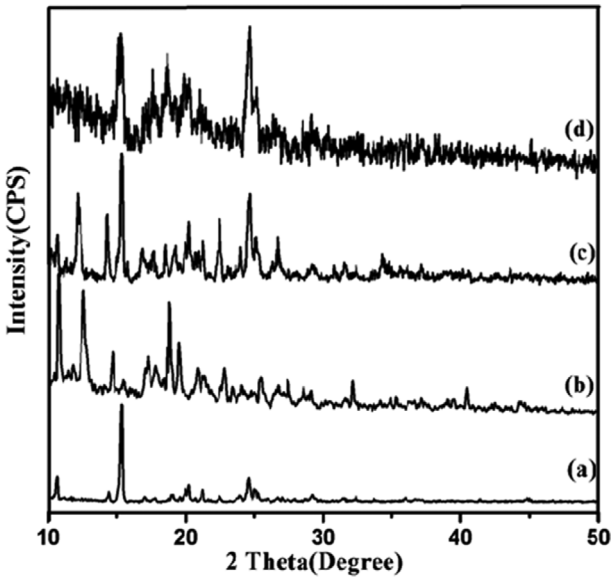

Fig. 7. Powder XRD patterns of (a) NP, (b) β-CD, (c) PM, and (d) NP : β-CD-ICs.

of NP substances, PM, and NP : β-CD-ICs examined under SEM. Images of the NP sample indicate a large-sized particle (Fig. 6(a)). Rock-like shaped crystals are seen in the pure β-CD sample (Fig. 6(b)). As can be seen in Figs. 6(c) and 6(d), PM and NP : β-CD-ICs have irregular shapes of varying sizes. PM shows the mixture of both the large-sized as well as rock-like crystals in the product, and it clearly represents the PM is simply mixed with the guest and hence no interaction between them to form ICs. But, ICs showed a completely irregular-shaped product and disappearance of the nature of NP and CD after complexation. Images like these clearly show ICs between NP and β-CD differences.

Additional evidence for an ICs between NP and β-CD was provided by X-ray diffraction patterns [45,46]. Fig. 7 shows the powder XRD patterns for NP, β-CD, PM, and NP : β-CD-IC and obtained in the 2θ range from 10 to 50. In powder XRD, the crystallinity of a sample can be evaluated and guests encapsulated with β-CD can be localized. Genuine ICs possess a more amorphous nature than crystalline. There were many crystalline peaks in the β-CD between 10 and 50, and the 2θ values of 8.96, 10.54, 12.46, 18.75, 22.58, 27.06, 31.86, and 34.59 were among them.

XRD patterns of NP (Fig. 7(a)) show different numbers of independent peaks depending on diffraction angles, such as 11.68, 12.44, 14.40, 15.32, 16.96, 17.76, 18.92, 20.20, 21.16, 22.40, 24.56, 26.96, 29.20, 32.36, and 35.92. As shown in Fig. 7(c), the PM peaks are 11.36, 12.12, 14.28, 15.32, 16.80, 17.68, 18.48, 20.20, 21.24, 22.44, 24.60, 26.68, 29.16, and 36.12. A unique XRD pattern was observed for ICs (Fig. 7(d)). Some of the low-intensity NP peaks were removed from ICs with β-CD.

The distinct pattern found in the ICs may be explained by the presence of NPs within the cavity of β-CDs. As a result of IC development, we see new peaks at 2θ values of 13.48, 19.84, 23.24, and 28.48 for the patterns of NP : β-CD-ICs. The discrepancies are indicative of an ICs forming between NP and β-CD in all of these patterns.

In the study of solid-state ICs between hosts and guests, ther-

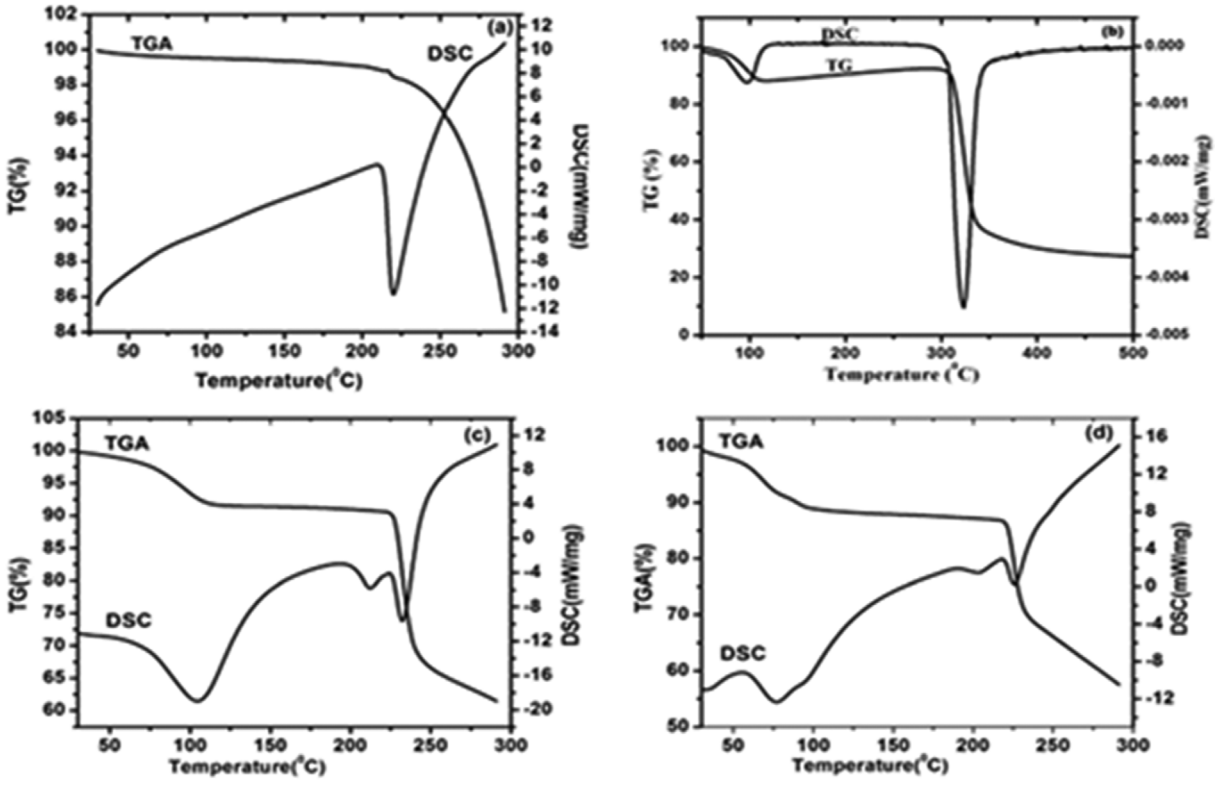

Fig. 8. TG/DSC curves of (a) NP, (b) β-CD, (c) PM, and (d) NP : β-CD-ICs.

mal behavior has been demonstrated to be an extremely useful tool. The thermal degradation property of the samples was studied using thermogravimetric methods (TG) [44]. In Fig. 8, we investigated changes in the thermal stability of NP, β-CD, PM, and NP : β-CD-ICs using TGA. When the NP was heated to 210.0 °C, it showed only one weight loss (Fig. 8(a)). A TGA curve of β-CD shows that it decomposes at 325.0 °C. The TGA curve indicates that the PM disintegrated at 225.0 °C. When the IC's TGA curve reaches 223.0 °C, it is deconstructed. After the development of ICs, the parameters relating to thermal degradation changed.

DSC thermograms are used to measure the rate at which NP and the NP : β-CD-ICs absorb heat. The article also provides qualitative and quantitative information regarding the physicochemical characteristics of the guests within β-CD ICs. A structure that contains an ICs typically results in the disappearance of an endothermic peak, the appearance of a new peak, a broadening or shifting of temperature indicating a new crystal lattice, melting, boiling, or sublimation points, and the broadening or shifting of temperature indicating a new crystal lattice [47]. The curves in Fig. 8 represent the DSC curves of NP, β-CD, PM, and NP : β-CD-ICs.

When guest molecules are inserted into the β-CD cavity, their melting, boiling, and sublimation points typically shift or vanish within the temperature range at which the cavity (or) lattice dissolves [48]. It was found that an abrupt endothermic peak developed at 220.1 °C, which was the melting point of the NP. A large endothermic peak can be identified on the DSC curve of β-CD, indicating a release of bound water; a second endothermic peak, around 327.1 °C, is primarily associated with the phase transition of β-CD. At 232.4 °C in the PM, a new endothermic peak is observed (Fig. 8(c)). This changes the strength of the endothermic peak (Fig. 8(d)) and shifts the peak position to 230.0 °C, which indicates the interaction of NP with β-CD in the PM. This result

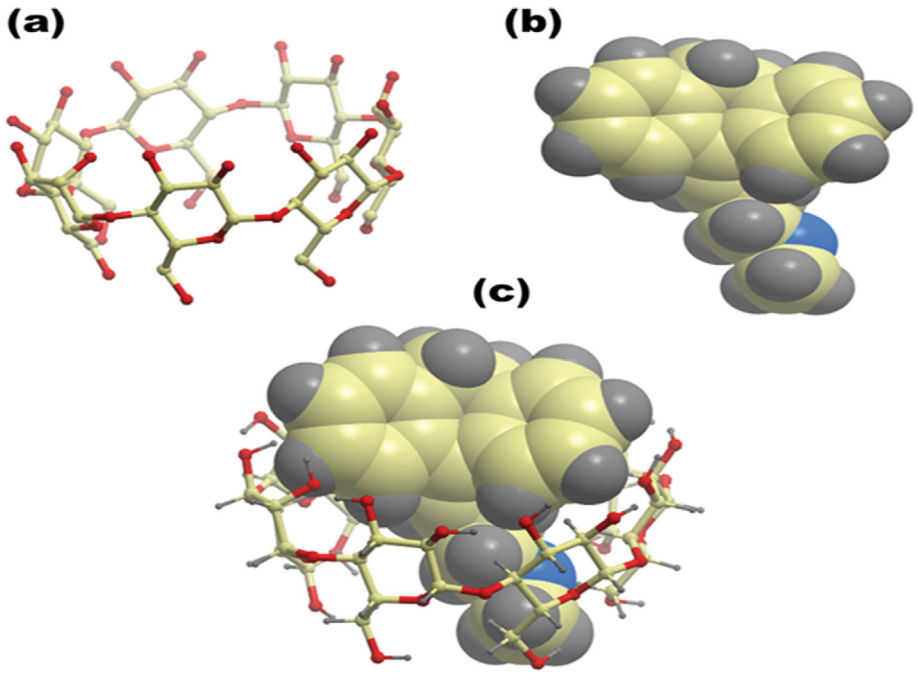

Fig. 9. Ball and stick representation of (a) β-CD (b) NP and (c) NP : β-CD-ICs.

Table 2. Scores of the top 10 docked models of NP : β-CD-ICs were computed using the Patch-Dock server

Model	Geometric shape complementarity score	Approximate interface area size of the complex Å^2	Atomic contact energy kcal/mol
1	3,824	427.80	−322.05
2	3,776	432.60	−329.75
3	3,772	441.40	−302.72
4	3,740	478.20	−338.11
5	3,738	425.90	−330.96
6	3,718	481.50	−330.41
7	3,710	466.80	−326.85
8	3,708	440.10	−322.56
9	3,642	460.20	−326.22
10	3,638	456.70	−325.37

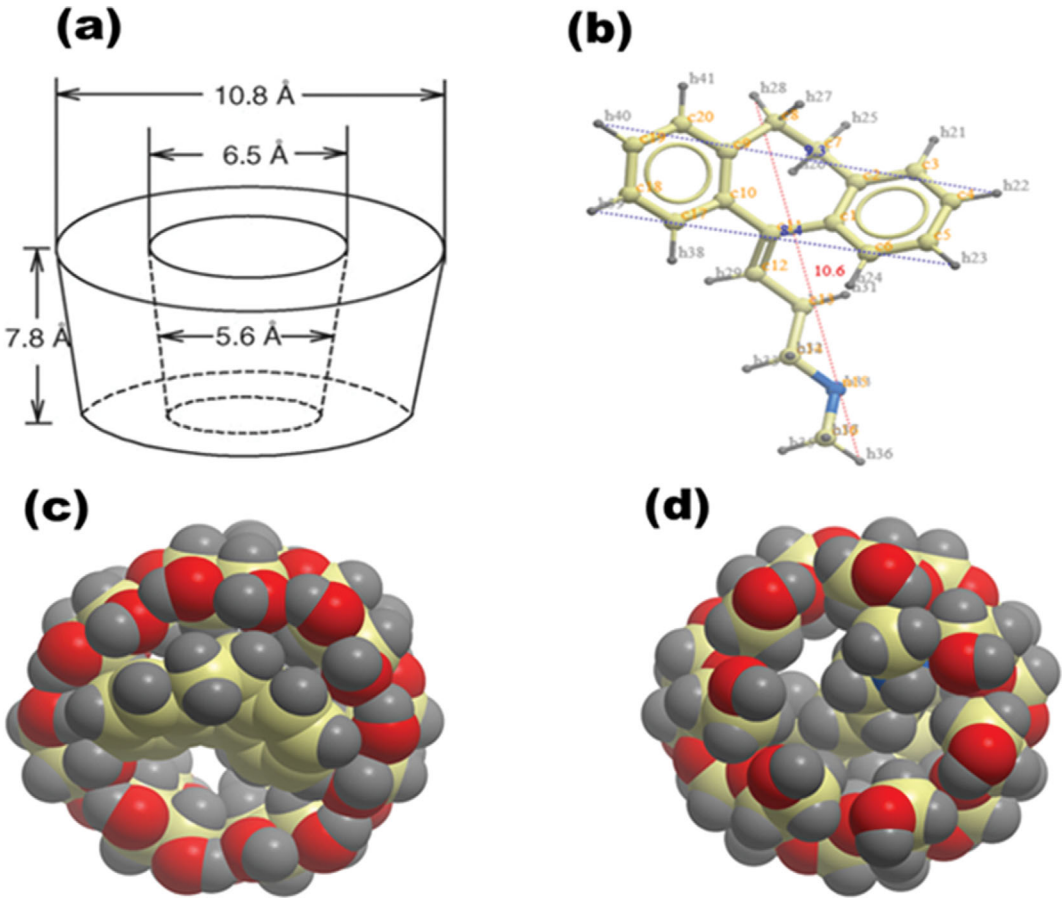

Fig. 10. Structure of (a) β-CD, (b) NP, (c) Front view structure NP : β-CD-ICs and (d) Back view the structure NP : β-CD-ICs.

illustrates the interaction of NP and β-CD in the ICs. This solid-state development of the NP : β-CD-ICs was validated through DSC.

3. Molecular Docking Approach for the NP : β-CD-ICs

From crystallographic databases, Figs. 9(a) and 9(b) show three-dimensional structures of β-CD and NP. NP was docked into the cavity of β-CD by using the Patch-Dock server. With the energetic parameters given by [49,50], the approximate area size of interfaces, and the atomic contact energy of NP : β-CD-ICs, the Patch-Dock server program was able to generate docked models of a variety of most likely structures (Table 2). In good agreement with experimental data, the docked NP : β-CD-ICs with a 1 : 1 model (Fig. 9(c)) with a geometric shape complementarity score of 3,824, approximately 427.80 square millimeters of contact area, and atomic contact energy of −322.05 kcal/mol had the highest geometric shape complementarity score and the largest contact area.

Table 3. *In-vitro* cytotoxic assay of NP and NP : β-CD-ICs on MCF-7 cell line

S. No	Name of the sample	Concentrations (%)	% of CT	CTC_{50} (μg/ml)
1	NP	100	80.44±0.6	7.67±0.2
		50	79.16±1.4	
		25	76.40±1.8	
		12.5	72.45±4.3	
		6.25	43.34±3.4	
2	NP : β-CD-ICs	100	80.07±0.5	9.04±0.3
		50	78.15±0.1	
		25	74.20±0.5	
		12.5	66.02±1.2	
		6.25	37.01±1.5	

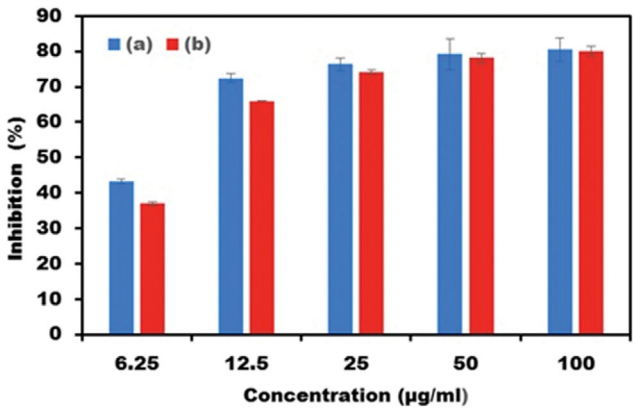

Fig. 11. Percentage inhibition for (a) NP and (b) NP : β-CD-ICs against MCF-7 cell line.

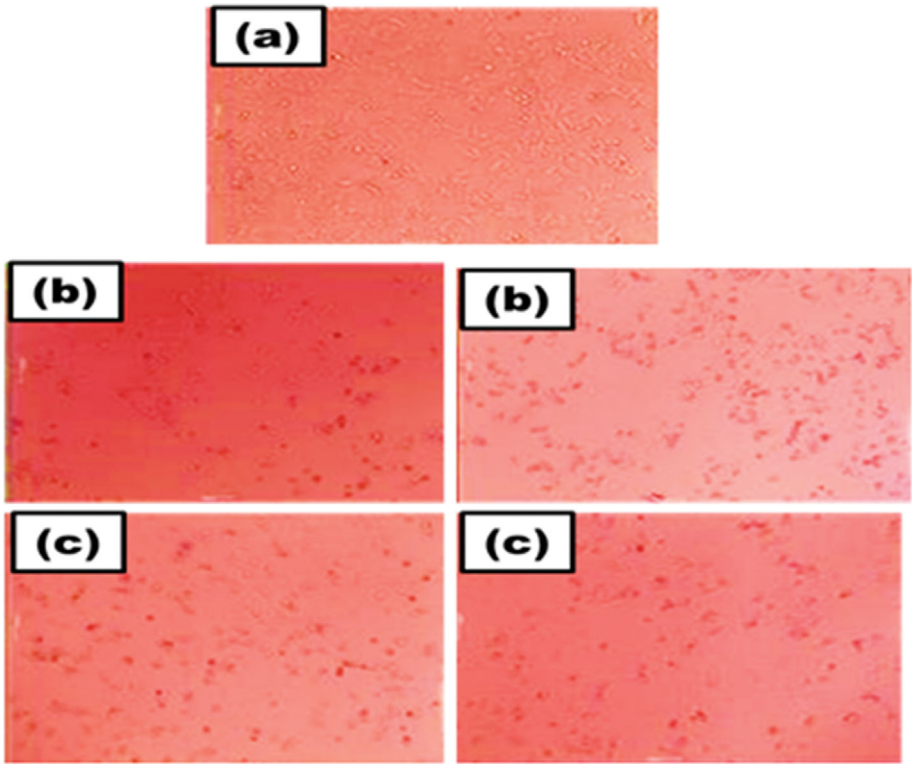

Fig. 12. Photos of (a) MCF-7 Control, (b) NP -500 & 1,000 μg/ml and (c) NP : β-CD-ICs -500 & 1,000 μg/ml.

The internal diameter of the β-CD is about 6.5 Å, while the height is 7.8 Å (Fig. 10(a)). The shape and dimensions of the β-CD cavity make it impossible for the NP molecule to be completely enclosed. As shown in Fig. 10(b), NP's overall height is 10.6 Å (i.e., the vertical distance between H_{28} and H_{23}), and the horizontal distance between H_{22} and H_{40} is 9.3 Å (as shown in Fig. 10(c)), the internal diameter of β-CD is 6.5 Å. Based on experimental results and docking studies, the side chain of NP is located within the cavity of the β-CD, as illustrated in Figs. 10(c) and 10(d).

4. *In-vitro* Cytotoxic Analysis on MCF-7 Cell Line

NP and NP : β-CD-ICs were examined *in-vitro* for their cytotoxic activity on the MCF-7 cell line using the MTT assay. Shown in Table 3 is the CT activity of two representative samples. The percentage of inhibition with cell viability is nearly identical when the chemical concentrations are adjusted from 6.25 to 100%, and this percentage does not change much as the concentration increases (Fig. 11). The two samples, fortunately, are effective on MCF-7 cells. The images in Fig. 12 are from the *in-vitro* cytotoxicity study. Viability is higher at higher concentration (Figs. 12(b) and 12(c)). As a result of the treatment with both samples, the cells are completely killed and enlarged. Additionally, CTC_{50} is less than 10 μg/ml is achieved for both the samples and ICs made a water-soluble anticancer agent. Because of this, it is feasible to use it in cancer treatment.

CONCLUSIONS

According to the results of this study, NP could be encapsulated with β-CD to form ICs. These BH plots provided evidence of the ICs' binding constant, as well as their 1 : 1 stoichiometric ratio. ΔG is a thermodynamic parameter derived from the changes in UV and fluorescence spectral outputs. ΔG is negative, indicating that NP inclusion occurs as an exothermic and spontaneous process. Furthermore, FT-IR, SEM, TG/DSC, and powder XRD analyses were performed to prove the presence of NP in the β-CD cavity. Thermal stability experiments in the ICs showed that NP was significantly more stable. To find the most energetically advantageous model of the ICs, docking studies were conducted. Experimentally and computationally, both the aliphatic and aromatic moiety of NP were partially embedded in the cavity of β-CD, with the aliphatic moiety located closer to the primary rim and the aromatic ring closer to the secondary rim. As well, the CTC_{50} values are less than 10 μg/ml; therefore, it is a potentially useful treatment for cancer.

DECLARATIONS

Ethical Approval

No humans or animals have been used in this research.

Competing Interests

The authors declare that they have no competing interests.

Author Contributions

Study conception and design: **Muthusamy Viswalingam**, Analysis and interpretation of results: **Muthusamy Viswalingam & Samikannu Prabu**, Software: **Krishnamoorthy Sivakumar**, Draft manuscript preparation: **Muthusamy Viswalingam**, Review & Edit-

ing: **Yong Rok Lee**, Review, Editing & Research Supervisor: **Rajaram Rajamohan.**

Funding

There is no funding for this research.

Availability of Data and Materials

The datasets used or analyzed during the current study are available from the corresponding author upon reasonable request.

REFERENCES

1. J. R. Hughes, *Addiction*, **101**, 1362 (2006).
2. E. Kirino and M. Gitoh, *Neuropsychiatr. Dis Treat.*, **7**, 723 (2011).
3. J. R. Dell and C. W. Butrick, *J. Reprod Med.,* **51**, 253 (2006).
4. X. Mao, T. Hou, B. Cao, W. Wang, Z. Li, S. Chen, M. Fei, R. Hurren, M. Gronda, D. Wu, S. Trudel and A. D. Schimmer, *Mol. Pharmacol.*, **79**, 672 (2011).
5. J. Ma, Y. Qiu, L. Yang, L. Peng, Z. Xia, L. N. Hou, C. Fang, H. Qi and H. Z. Chen, *J. Neuro-Oncol.*, **101**, 41 (2011).
6. P. Kabolizadeh, B. J. Engelmann, N. Pullen, J. K. Stewart, J. J. Ryan and N. P. Farrell, *J. Biol. Inorg. Chem.*, **17**, 123 (2012).
7. V. Muthusamy, S. Prabu, S. Krishnamoorthy and R. Rajaram, *J. Macromol. Sci. Part A.*, **53**, 781 (2016).
8. V. Muthusamy, S. Prabu, S. Krishnamoorthy and R. Rajaram, *Ins. Sci. Tech.*, **44**, 651 (2016).
9. K. A. Parker, S. Glaysher, J. Hurren, L. A. Knight, D. McCormick, A. Suovouri, V. Amberger-Murphy, G. J. Pilkington and I. A. Cree, *Anticancer Drugs*, **23**, 65 (2012).
10. P. Chih-Chuan, C. F. Shaw, J. K. Huang, C. C. Kuo, D. H. Kuo, P. Shieh, T. Lu, W. C. Chen, C. M. Ho and C. R. Jan, *Drug Dev. Res.*, **71**, 323 (2010).
11. E. S. Sinem and A. Umit, *J. Sol. Chem.*, **48**, 1535 (2019).
12. A. Umit, *J. Appl. Spec.*, **88**, 838 (2021).
13. E. S. Sinem and A. Umit, *Inorg. Chem. Comm.*, **114**, 107820 (2020).
14. F. W. Lichtenthaler and S. Immel, *Starch/Starke*, **48**, 145 (1996).
15. F. Paola and M. Iolandade, *J CO_2 Util.*, **44**, 101397 (2021).
16. Y. Tingxuan, J. Mengru, S. Yuxi, Y. Tingyuan, Z. Jie, Z. Huiwen and W. Zhixiang, *J. Incl. Phen. Macro. Chem.*, **96**, 285 (2020).
17. H. Xie, H. Z. Wangb, Y. Mac Li, Y. Xiaob and J. Hanb, *Spectrochim. Acta Part A*, **62**, 197 (2005).
18. J. B. Chao, H. B. Tong, D. S. Liu and S. P. Huang, *Spectrochim. Acta Part A*, **64**, 166 (2006).
19. K. Kuppusamy, X. Chao, R. Ming, F. Chunying, B. Victor, C. Guo, Z. Dayang, Z. Zhihui, S. Dan, Y. Xingke, Y. Jiabin, H. Taotao, W. Wanhua, J. C. Jason and Y. Cheng, *iScience*, **23**, 100927 (2020).
20. A. A. Elbashir, N. F. A. Dsugi and H. Y. Aboul-Enein, *J. Fluoresc.*, **24**, 355 (2014).
21. J. B. Chao, H. B. Tong, S. P. Huang and D. S. Liu, *Spectrochim. Acta Part A.*, **60**, 161 (2005).
22. L. Liu and Q. X. Guo, *J. Inc. Phenom. Macrocyclic Chem.*, **42**, 1 (2002).
23. S. Saha, H. Agarwalla, H. Gupta, M. Baidya, E. Suresh, S. K. Ghosh and A. Das, *Dalton Trans.*, **42**, 15097 (2013).
24. R. Rajamohan, S. Kothai Nayaki, K. Sivakumar and M. Swaminathan, *J. Lumin.*, **68**, 245 (2015).
25. S. Prabu, N. Abdul Samad, N. Afiqah Ahmad, K. Jumbri, M. Raoov, N. Yani Rahim, S. Kanagesan and M. Sharifah, *Carb. Res.*, **497**, 108138 (2020).
26. D. Duhovny, R. Nussinov and H. J. Wolfson, Proceedings of the 2nd Workshop on Algorithms in Bioinformatics (WABI), Rome, Italy, Lecture Notes in Computer Science, *Springer Verlag*, **2452**, 185 (2002).
27. M. L. Connolly, *J. Appl. Crystallogr.*, **16**, 548 (1983).
28. C. Zhang, G. Vasmatzis, J. L. Cornette and C. DeLisi, *J. Mol. Biol.*, **267**, 707 (1997).
29. M. Murugan, A. Anitha, K. Sivakumar and R. Rajamohan, *J. Mol. Liq.*, **325**, 115157 (2020).
30. V. Ramamurthy and D. F. Eaton, *Acc Chem. Res.*, **21**, 300 (1988).
31. M. Hoshino, M. Imamura, K. Ikehara and Y. Hama, *J. Phys. Chem.*, **85**, 1820 (1981).
32. K. A. Al-Hassan, U. K. A. Klein and A. Suwaiyan, *Chem. Phys. Lett.*, **212**, 581 (1993).
33. D. W. Cho, Y. H. Kim, S. G. Kong, M. Yoon and D. Kim, *J. Chem. Soc. Faraday Trans.*, **92**, 29 (1996).
34. H. A. Benesi and J. H. Hildebrand, *J. Am. Chem. Soc.*, **71**, 2703 (1949).
35. J. Szejili and T. Osa, *Pergamon Press Oxford*, **3**, 253 (1996).
36. L. Chandrabose, S. Krishnamoorthy and R. Rajaram, *J. Macromol. Sci. Part A.*, **54**, 402 (2017).
37. R. Rajaram, M. Sonaimuthu, A. Sekar, C. Eun Ha, M. Fatiha, L. Neour and L. Yong Rok, *J. Mol. Liq.*, **366**, 120297 (2022).
38. A. Saxena, G. Tewari and S. A. Saraf, *Braz. J. Pharm. Sci.*, **47**, 887 (2011).
39. W. Zielenkiewicz, M. Kozbiał, B. Golankiewicz and J. Poznanski, *J. Therm. Anal. Cal.*, **101**, 555 (2010).
40. P. R. Von, C. Sepulveda Carreno, J. Rodriguez-Baeza and J. B. Alderete, *Química Nova*, **23**, 749 (2000).
41. T. Loftsson, K. Matthiasson and M. Masson, *Int. J. Pharm.*, **262**, 101 (2003).
42. H. M. Marques, J. Hadgraft and I. W. Kellaway, *Int. J. Pharm.*, **63**, 259 (1990).
43. R. Periasamy, R. Rajamohan, S. Kothainayaki and K. Sivakumar, *J. Mol. Str.*, **1068**, 155 (2014).
44. R. Rajaram, M. Sonaimuthu, A. Sekar, M. Fatiha, L. Neour, M. Kuppusamy and L. Yong Rok, *J. Pharm. Biomed. Anal.*, **221**, 115057 (2022).
45. G. Narayanan, R. Boy, B. S. Gupta and A. E. Tonelli, *Polymer Testing*, **62**, 402 (2017).
46. P. Mura, *J. Pharm. Biomed. Anal.*, **113**, 226 (2015).
47. S. Uppal, K. Kaur, N. Rajendra Kumar, K. Rachna Singh and S. K. Mehta, *Ultrason Sonochem.*, **39**, 25 (2017).
48. H. M. Marques, J. Hadgraft and I. W. Kellaway, *Int. J. Pharm.*, **63**, 259 (1990).
49. D. Schneidman-Duhovny, I. Yuval, N. Ruth and H. J. Wolfson, *Nuc. Acids Res.*, **33**, 363 (2005).
50. M. L. Connolly, *Science*, **221**, 709 (1983).